EFFECTS OF SOIL INHOMOGENEITY ON SEEPAGE BEHAVIOR WITHIN EMBANKMENTS

Koji Nakashima*, Katsuyuki Kawai, Hideaki Yoshida

Kindai University, 3-4-1 Kowakae, Higashiosaka, Osaka, Japan

*Corresponding author: knakashima@civileng.kindai.ac.jp

(Received: January 5, 2023; Revised: May 05, 2023; Accepted: May 19, 2023)

Abstract - Heavy rain events that accompany recent climate change, have triggered disasters of embankment structures, such as road embankment and levee. Internal erosion, which is the migration of soil particles following seepage flow, causes inhomogeneity of the soil properties of the embankment. However, there are very few studies investigating the effects of soil inhomogeneities on the seepage behavior of groundwater within embankment. In this study, small-scale modelling tests were performed under repeated seepage flow histories. As a result, the groundwater table gradually increased in accordance with the number of seepage repetition. Modelling the fluctuation of permeability due to internal erosion following seepage flow was additionally performed using the soil/water/air coupled finite element analysis, and seepage behavior was investigated. In these analyses, the lower permeability of the toe of embankment was shown to possibly cause an increase in upward water pressure.

Key words - Soil inhomogeneity; seepage behavior; road embankment; levee; internal erosion.

1. Introduction

In Japan, embankment damage has increased due to flooding events accompanying torrential rain. River levees and road embankments are one type of embankment structure that has the important role of protecting human lives, property, and social infrastructure. In recent years, river levees have often been found to fail due to the development of piping following seepage. For example, a river levee along the Yabe River failed due to the development of piping during the flood event following heavy rains in Northern Kyusyu, Japan in 2012 [1]. Recently, road embankment damage, caused not only by earthquakes but also by rainfall, has frequently occurred, such as the losses that occurred in the 2015 heavy rain disaster in the Kanto and Tohoku districts. Embankment structures are usually constructed by compacting various natural soils. Therefore, inhomogeneity of material properties, such as density and particle size distribution, is potentially inevitable. Additionally, they are semi-permanently utilized, and hence, it is assumed that material and physical properties spatially change from their initial condition due to the seepage history of rain and river water.

Internal erosion, which is the migration of soil particles following seepage flow, is well known as a phenomenon which induces soil inhomogeneity. The formation of highly permeable layers due to internal erosion may cause the development of piping. Moreover, clogging from the migrated soil particles increases the possibility of inducing water table level rise within the embankment. Several laboratory experiments to reveal the mechanism and the triggers of internal erosion have previously been performed. They have mainly been conducted with elemental specimens, and hence, there were few cases investigating internal erosion behavior at the model test level. Horikoshi et al. [2] performed a series of embankment model tests under constant boundary head conditions. They revealed the eroded soil moves by both seepage flow and gravitational force, which causes a decrease in the permeability of the whole embankment.

In this study, a modelling test was performed with the small-scale embankment model. Seepage behavior within the embankment was investigated under the repeated flooding histories. Additionally, assuming the permeability within the embankment varied due to soil inhomogeneity caused by internal erosion, seepage flow analysis was performed using the soil/water/air coupled finite element method.

2. Embankment modelling test under repeated seepage histories

2.1. Test material

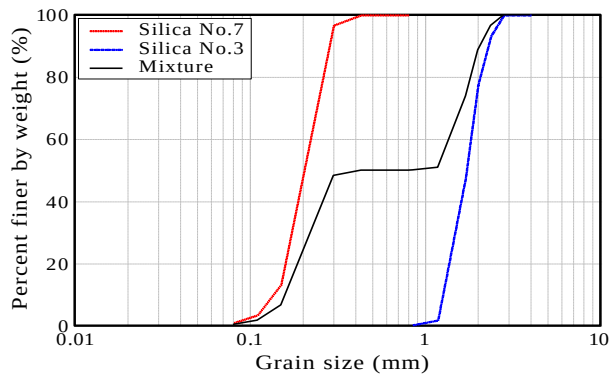

Figure 1. *Particle size distribution curve of test material*

The test material, which included fine and coarse fractions, was prepared by blending No.3 and No.7 silica sands. The particle size distribution (PSD) curve of the test material is shown in Figure 1. PSD is often used to evaluate the vulnerability of the soil material to internal erosion. For example, Kenny and Lau [3] proposed the filter criterion that classifies the instability of soils against seepage. The internal instability can be predicted by two parameters, H and F, which are obtained from the PSD, as illustrated in Figure 2. Soils which have $(H/F)_{min}$ of more than 1.3 are classified as stable. The test material has $(H/F)_{min}$ of 0.05. Alternatively, the gap ratio proposed by Chang and Zhang [4], is useful for the soils which have gap grading. This is defined as the ratio of the greater particle size d_{max} to the finer particle size d_{min}. Soils which have less fines content (<10%) are classified as

stable when G_r<3.0. The gap ratio of the test material was G_r=4.72. According to these approaches, the test material is potentially vulnerable to seepage. These material properties are summarized in Table 1.

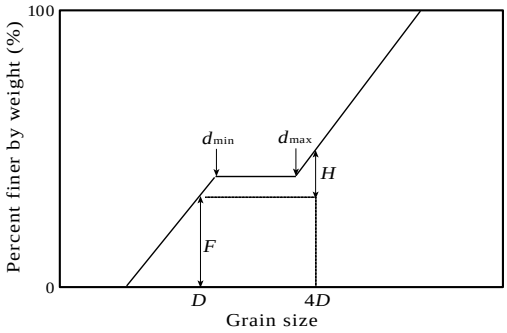

Figure 2. *Definition of internal erosion parameters*

Table 1. *Material properties and internal erosion parameters*

Specific gravity of soil particles G_s	Uniformity coefficient U_c	Maximum void ratio e_{max}	Minimum void ratio e_{min}	$(H/F)_{min}$	Gap ratio G_r
2.60	8.81	0.83	0.48	0.05	4.72

2.2. Model preparation and test procedures

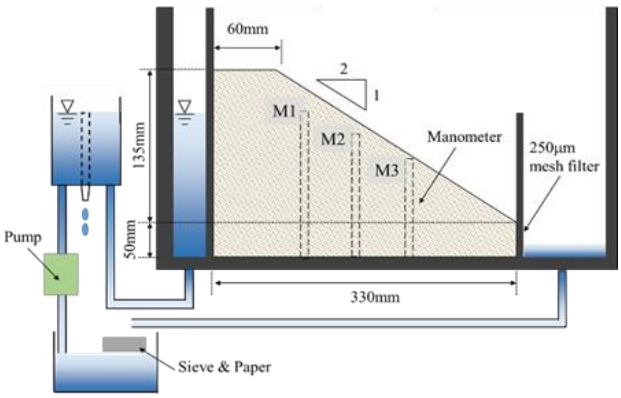

Figure 3. *Experiment configuration*

Figure 3 illustrates an overview of the test equipment. The embankment model was constructed by compaction. To prevent soil separation during model preparation, pre-calculated water was added to the test material until a moisture content of w=10%. The soil material is compacted of five layers at a target relative density of D_r = 60%. After compaction, the excess sands were scraped off using pallet knives, to be the geometry of 185mm in height, 60mm in crest width, 330mm in base width, and 1:2 in a slope. Three manometers were attached to the bottom of the base material through the box. A mesh filter was fixed in a retaining plate of the outlet side to allow the washing away of finer particles. A digital camera was set up to capture the photos of the manometers during the test. The ground water level within the embankment model was specified by continuously tracking the height of the manometers from the photos. Water supply using a pump kept a constant water level at the upper tank and the top of the embankment. Repeated maximum water levels between 90% and 0% of the embankment height were set over a period of 5 days, as shown in Figure 4. Drainage water from the embankment toe was collected, and turbidity was measured.

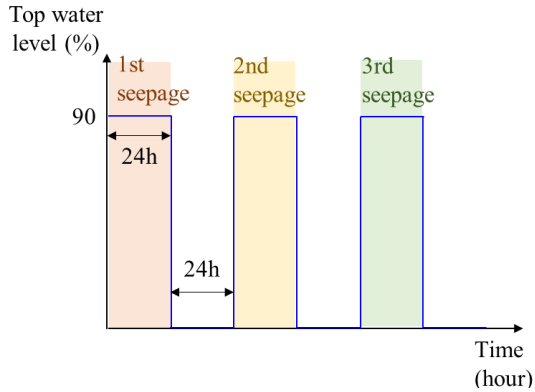

Figure 4. *Hydraulic condition*

2.3. Test results

The water level measurements for each manometer during the seepage test are shown in Figure 5. As observed in the figure, the water levels show an increase in an accordance with the number of seepage repetition. They also slightly increase for 24 hours during each cycle. This means the permeability of the embankment gradually decreased with the seepage history. Figure 6 represents the results of turbidity during the test. The turbidity gradually decreased in each cycle. Thereafter, it slightly increased; however, this was negligible compared to the initial decreasing fluctuation. To summarize the above results, finer particles were washed away from the embankment at the initial state. As internal erosion progressed, clogging due to migrated particles led to the formation of an area of lower permeability within the embankment.

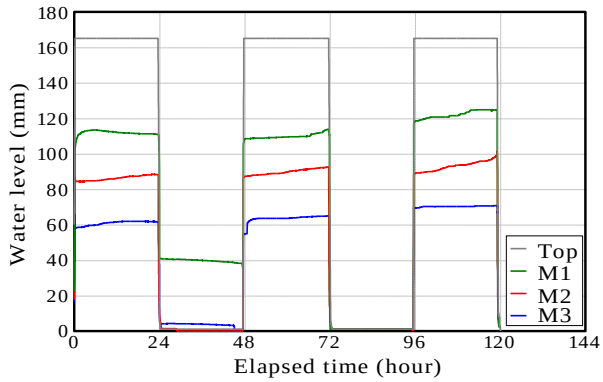

Figure 5. *Time histories of water level*

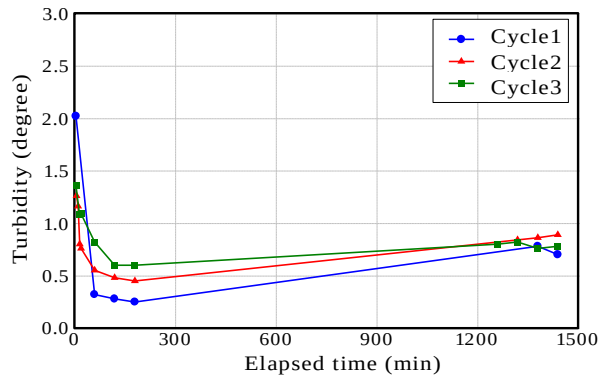

Figure 6. *Turbidity during flooding*

3. Modelling of soil inhomogeneity using finite element analysis

The previous section confirmed that internal erosion influences seepage behavior within the embankment. In this section, a soil/water coupled finite element analysis was conducted to capture the seepage trend due to the soil inhomogeneity within the embankment.

3.1. Numerical model

The soil/water/air coupled finite element analysis code DACSAR-MP [5] was used for the analysis. The constitutive model proposed for unsaturated soil [6] was introduced. Effective stress is given by the following equation.

$$\boldsymbol{\sigma}' = \boldsymbol{\sigma}^{net} + p_s\mathbf{1} \quad (1)$$

$$\boldsymbol{\sigma}^{net} = \boldsymbol{\sigma} - p_a\mathbf{1},\ p_s = S_e s \quad (2)$$

$$s = p_a - p_w,\ S_e = \frac{S_r - S_{rc}}{1 - S_{rc}} \quad (3)$$

Where, $\boldsymbol{\sigma}'$ is the effective stress tensor; $\boldsymbol{\sigma}^{net}$ is the net stress tensor; $\mathbf{1}$ is the unit tensor; $\boldsymbol{\sigma}$ is the total stress tensor; p_s is suction stress; p_a is the pore air pressure; p_w is the pore water pressure; s is suction; S_e is the effective degree of saturation; S_r is the degree of saturation; and S_{rc} is the degree of residual saturation at $s \to \infty$. The constitutive relationship is given by the following equations.

$$\boldsymbol{\sigma}' = \boldsymbol{D}:\boldsymbol{\varepsilon} - \boldsymbol{C}\cdot\dot{S}_e \quad (4)$$

Where, $\mathbf{D}$ is the elastoplastic rigidity matrix; $\boldsymbol{\varepsilon}$ is the strain tensor; and $\mathbf{C}$ is the tensor representing rigidity changes resulting from unsaturated conditions. Continuity equations of pore water and pore air are given by the following equations.

$$n\dot{S}_r - S_r\dot{\varepsilon}_v + div\tilde{\boldsymbol{v}}_{\boldsymbol{w}} = 0 \quad (5)$$

$$(1 - S_r)\dot{\varepsilon}_v + n\dot{S}_r - n(1 - S_r)\frac{\dot{p}_a}{p_a + p_0} - div\tilde{\boldsymbol{v}}_a = 0 \quad (6)$$

Where, n is porosity; $\tilde{\mathbf{v}}_w$ and $\tilde{\mathbf{v}}_a$ are relative velocities of pore water and pore air; ε_v is volumetric strain; and p_0 is the atmospheric pressure. The specific hydraulic conductivity under unsaturated conditions was determined by Mualem's equation as below.

$$k_{rw} = S_e^{\frac{1}{2}}\left[1 - \left(1 - S_e^{\frac{1}{m}}\right)^m\right]^2 \quad (7)$$

Where, k_{rw} is the specific hydraulic conductivity, and m is Mualem's coefficient. Kawai et al. [7] proposed a soil-water characteristics curve model that can express the influence of hysteresis between drying and wetting processes. In this study, the model was introduced to express unsaturated soil characteristics.

3.2. Analytical embankment model

Table 2 shows the material parameters input for the analysis. λ and k are compression and swelling index. M is critical stress ratio. They are obtained from the soil tests. The parameters n_E, a and n_S determine the increase in the yield stress with change in degree of saturation, and are given by fitting. The parameters k_x and k_y are the hydraulic conductivity in each direction. The hydraulic conductivity obtained from the constant head permeability test was used without considering anisotropy. Figure 7 shows the analysis elements and boundary conditions that mimic the experimental embankment model. In this study, the analysis proceeded as follows. First, a water head boundary of 0m at the embankment toe and the permeable boundary of 0kPa at the slope were set. Subsequently, the top water level rise was simulated by increasing the water head boundary by 3cm per minute up to 50% of the embankment height. The water pressure at the center of the element composing the slope was then monitored. The hydraulic conductivity changed when water pressure converted from a negative to a positive value below the infiltration surface, as illustrated in Figure 8. To simulate the heterogeneous embankment, seepage analyses were performed for two cases; one in which the hydraulic conductivity increased 100 times (Case1: 0.06m/day → 6.0m/day) and the other in which it decreased to 1/100 times (Case2: 0.06m/day → 0.0006m/day).

Table 2. *Inputted material parameters*

λ	k	M	m	n_E
0.11	0.01	1.34	0.80	1.0
a	n_s	S_{rc}	k_x (m/day)	k_y (m/day)
1.0	1.0	0.15	0.06	0.06

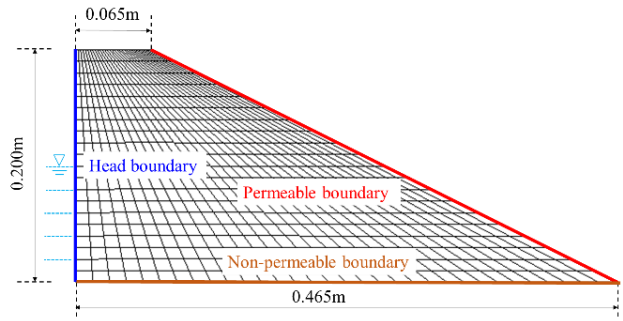

Figure 7. *Analysis elements and boundary conditions*

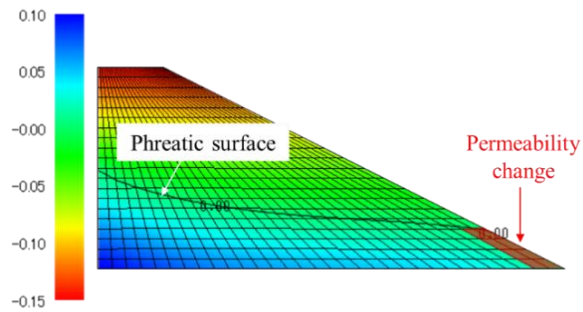

Figure 8. *Region of change in permeability*

3.3. Analysis results

Figure 9 shows the distribution of water pressure and equipotential lines, obtained 3 hours after the hydraulic conductivity changed. For comparison, the case with constant permeability is also shown. For Case 1, the water pressure distribution shows a similar trend to the case with constant coefficient of permeability. Whereas, for Case 2, the region of high-water pressure extends toward the embankment toe compared to the other two cases. Subsequently, comparing the total hydraulic head distribution, Case 2 significantly differs from the other two

cases. Higher potentials at the toe and extremely narrow spacing between potential lines were observed, which implies the hydraulic gradient increased. Additionally, from the appearance of the equipotential lines, upward flow is expected to occur around the toe. The upward water pressure may lead to the instability of the soil.

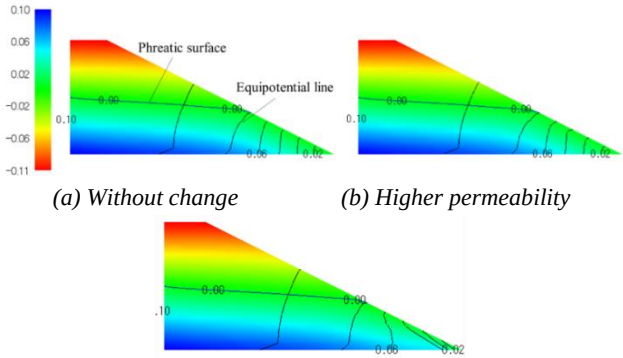

(a) Without change *(b) Higher permeability*

(b) Lower permeability

Figure 9. *Distribution of water pressure and equipotential lines (after forming the inhomogeneous region)*

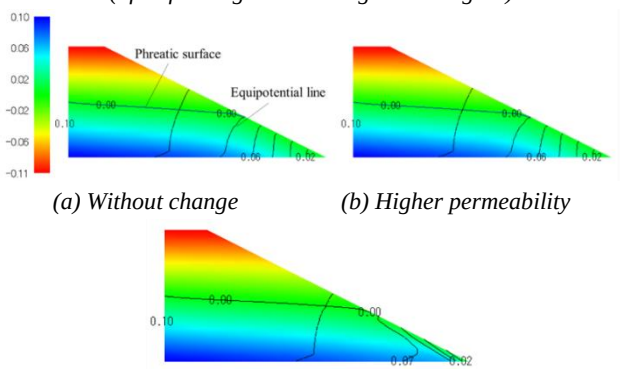

(a) Without change *(b) Higher permeability*

(b) Lower permeability

Figure 10. *Distribution of water pressure and equipotential lines (after progression of the inhomogeneous region)*

After the change in the hydraulic conductivity, the area of positive water pressure was extended on the slope in about one hour. The hydraulic conductivity of the element was newly changed, whereby progression of the inhomogeneous region was simulated. Figure 10 shows the results of analysis after two hours. For Case 2, the spacing of the potential lines became increasingly narrow, whereby the hydraulic gradient significantly increased. As observed in the experimental results, less permeability due to the progress of internal erosion has a high possibility of causing embankment instability. Whereas, increasing permeability does not affect the seepage behavior within the embankment.

4. Conclusion

In this paper, a small-scale embankment model test was performed under repeated flooding histories. Additionally, seepage flow analysis, which simulated soil inhomogeneity due to internal erosion, was performed. The following conclusions were drawn.

(1) The groundwater table gradually increases in accordance with the number of seepage repetition, which means the permeability of the embankment decreases with seepage history.

(2) The turbidity gradually decreases in each cycle. This indicates that clogging due to migrated fine particles leads to the formation of the lower permeability area of the embankment.

(3) From the results of seepage analysis, in cases where a higher permeability area was formed, the water pressure distribution shows a similar trend to the case with constant hydraulic conductivity. Whereas, in the case where a lower permeability area was formed due to particle clogging, the hydraulic gradient increased. Furthermore, in this case, the upward water pressure may lead to the instability of soils.

Acknowledgments: This research is funded by JSPS KAKENHI (No. 21K14244).

REFERENCES

[1] Y. Honjo, H. Mori, M. Ishihara and Y. Otake, *"*On The Inspection of River Levee Safety in Japan by MLIT", *Geotechnical Safty and Risk V*, pp. 873-878, 2015. doi:10.3233/978-1-61499-580-7-873.

[2] K. Horikoshi and A. Takahashi, "Suffusion-induced change in spatial distribution of fine fractions in embankment subjected to seepage flow", *Soils and Foundations*, vol. 55, no. 5, pp. 1293-1304, 2015. https://doi.org/10.1016/j.sandf.2015.09.027

[3] T. C. Kenney and D. Lau, "Internal stability of granular filters", *Canadian Geotechnical Journal*, vol. 22, no. 2, pp. 215-225, 1985.

[4] D. S. Chang and L. M. Zhang, "Extended internal stability criteria for soils under seepage", *Soils and Foundations*, vol. 53, no. 4, pp. 569-583, 2013. https://doi.org/10.1016/j.sandf.2013.06.008

[5] Y. Sugiyama, K. Kawai and A. Iizuka, "Effects of stress conditions on B-value measurement", *Soils and Foundations*, vol. 56, no. 5, pp. 848-860, 2016. https://doi.org/10.1016/j.sandf.2016.08.009

[6] S. Ohno, K. Kawai and S. Tachibana, "Elasto-plastic constitutive model for unsaturated soil applied effective degree of saturation as a parameter expressing stiffiness", *Journal of Japan Society of Civil Engineers*, vol. 63, no. 4, pp. 1132-1141, 2007 (in Japanese). DOI:10.2208/jscejc.63.1132.

[7] K. Kawai, A. Iizuka, E. Hayakawa and W. Wang, "Non-uniform settlement of compacted earth structures caused by the deformation characteristics of unsaturated soil on wetting", *Soils and Foundations*, vol. 47, no. 2, pp. 195-205, 2007.